Title

Conformation-Directed Formation of Self-Healing Diblock Copolypeptide Hydrogels via Polyion Complexation.

Journal

Journal of the American Chemical Society, 139(42)

ISSN

0002-7863

Authors

Sun, Yintao
Wollenberg, Alexander L
O'Shea, Timothy Mark
et al.

Publication Date

2017-10-01

DOI

10.1021/jacs.7b08190

Peer reviewed

Conformation directed formation of self-healing diblock copolypeptide hydrogels via polyion complexation

Yintao Sun[a], Alexander L. Wollenberg[b], Timothy Mark O'Shea[c], Yanxiang Cui[d], Z. Hong Zhou[d,e], Michael V. Sofroniew[c] and Timothy J. Deming[a,b,d]*

[a] Department of Bioengineering, University of California, Los Angeles, CA 90095

[b] Department of Chemistry and Biochemistry, University of California, Los Angeles, CA 90095

[c] Department of Neurobiology, David Geffen School of Medicine, University of California, Los Angeles, Los Angeles, CA 90095

[d] California NanoSystems Institute, University of California, Los Angeles, CA 90095

[e] Department of Microbiology, Immunology and Molecular Genetics, University of California, Los Angeles, Los Angeles, CA 90095

Abstract Synthetic diblock copolypeptides were designed to incorporate oppositely charged ionic segments that form β-sheet structured hydrogel assemblies via polyion complexation when mixed in aqueous media. The observed chain conformation directed assembly was found to be required for efficient hydrogel formation, and provided distinct and useful properties to these hydrogels including self-healing after deformation, microporous architecture, and stability against dilution in aqueous media. While many promising self-assembled materials have been prepared using disordered or liquid coacervate polyion complex (PIC) assemblies, the use of ordered chain conformations in PIC assemblies to direct formation of new supramolecular morphologies is unprecedented. The promising attributes and

unique features of the β-sheet structured PIC hydrogels described here highlight the potential of harnessing conformational order derived from PIC assembly to create new supramolecular materials.

Introduction

The concept of conformation directed assembly has been widely utilized in the design and preparation of ordered supramolecular structures.[1-3] In particular, assemblies containing peptides and polypeptides often take advantage of hydrophobic and H-bonding interactions between ordered chain conformations in these molecules, e.g. α-helices and β-strands, to produce materials with advantageous properties, such as defined morphology or enhanced stability.[4] Polypeptide containing block copolymer assemblies, such as micelles, vesicles, and hydrogels, have also been prepared using polyion complexes (PICs),[5,6] where oppositely charged chain segments aggregate and phase separate upon mixing in aqueous media. In these systems, as well as those based on other synthetic polymers, formation of unstructured, liquid PIC coacervate domains is common and often desired. Fluidity in PIC coacervates can assist rapid complex formation and equilibration, while formation of solid β-sheet structures can lead to irregular assemblies with less desirable properties.[5-8] In a contrarian approach, we sought to generate conformational order in polypeptides using PIC assembly to direct supramolecular assemblies into unprecedented morphologies with desirable properties. Using knowledge that certain homochiral polypeptide PICs form β-sheet aggregates,[9-11] we designed diblock copolypeptides incorporating such oppositely charged ionic segments that were able to form supramolecular hydrogels via PIC assembly in aqueous media. Since these hydrogels assemble via ordered chain conformations, different from other PIC hydrogels that require triblock copolymers and utilize disordered confromations,[12-15] they possess distinct properties such as rapid recovery after stress and microporous architecture. Furthermore, these PIC diblock copolypeptide hydrogels (DCH_{PIC}) possess certain advantages over hydrophobically

assembled DCH[16] in that they are resistant to dilution in aqueous media, and are readily prepared at high concentrations for increased hydrogel stiffness.

Aqueous PIC assembly of block copolymers containing both non-ionic and oppositely charged ionic segments has been used to prepare a diverse array of micelles, vesicles, and hydrogels.[5,6,17] Most polypeptide containing PIC assemblies utilize polyethylene glycol (PEG) chains as hydrophilic non-ionic segments, as well as ionic polypeptide segments that form disordered or liquid coacervate immiscible phases.[5,6,12-15,18,19] The resulting lack of internal order in the complexes tends to favor formation of spherical assemblies as found in diblock copolymer micelles and triblock copolymer hydrogels. [5,6,12-15,18,19] Kataoka's lab has further shown that use of polypeptide segments that are long relative to PEG chain lengths results in formation of PICsome vesicular membrane assemblies.[20,21] In the few examples where internal order has been incorporated into polypeptide PIC assemblies, via use of ionic α-helical segments[8] or by β-sheet formation during assembly,[7,22] only minimal perturbation of spherical micelle formation or slowed formation of micelles with increased polydispersity was observed. While there are examples of peptides and polypeptides where β-sheet structures are used to direct formation of self-assembled materials, these all rely on other components, such as hydrophobic and non-ionic residues to drive β-sheet formation.[23,24] To the best of our knowledge, there are no reports demonstrating formation of new supramolecular morphologies that rely on assembly of polyelectrolyte segments into β-sheet rich domains.

The complexation of oppositely charged polypeptide electrolytes in aqueous media has been under study for many decades.[5,6] Blout and Idelson were the first to report that mixture of homochiral poly(L-lysine-HCl), **K**, and poly(L-glutamate-Na), **E**, in water gave rise to phase separation of PICs rich in β-sheet content.[9] Later studies confirmed this result and showed that while the mixture of L-lysine and L-glutamate homopolymers formed β-sheets, other combinations with L-ornithine or L-aspartate homopolymers gave only disordered PICs.[10] This observation led to the hypothesis that interactions

between hydrophobic side-chains, which are longer in lysine and glutamate, helped stabilize formation of the observed PIC β-sheet structure. More recently, the importance of chirality was shown by studies where replacement of one or both of the homochiral **K** and **E** components with racemic equivalents. i.e. ***rac*-K** or ***rac*-E**, led to formation of liquid coacervates instead of solid β-sheets.[7,22] Although most designs for polypeptide PIC assemblies favor formation of complexes with disordered internal structure,[5,6] we sought to take advantage of the ability of homochiral **K** and **E** based PICs to form ordered β-sheet assemblies.

The design of DCH_{PIC} was developed from our understanding of hydrophobically assembled amphiphilic DCH. In these materials, the combination of long, hydrophilic segments with disordered conformations, and shorter hydrophobic segments with either α-helical or β-sheet ordered conformations, e.g. poly(L-lysine-HCl)$_{180}$-*block*-poly(L-leucine)$_{20}$, $\mathbf{K_{180}L_{20}}$ or poly(L-lysine-HCl)$_{160}$-*block*-poly(L-valine)$_{40}$, $\mathbf{K_{160}V_{40}}$, respectively, was found to direct their assembly in water into anisotropic structures that branch and entangle to give 3D hydrogel networks.[16] The key molecular elements required for hydrogel formation are the conformation directed assembly of ordered hydrophobic segments into anisotropic structures instead of spherical micelles, and long, disordered hydrophilic chains that sterically limit packing of hydrophobic segments into tape-like assemblies as opposed to flat 2D membranes. To create DCH_{PIC}, we sought to test if the ordered hydrophobic component in amphiphilic DCH, e.g. β-sheet forming **V** segments, could be replaced with β-sheet PICs formed from mixing of **K** and **E** chains (Figure 1). Concurrently, it was also necessary to replace the disordered, ionic hydrophilic component of amphiphilic DCH, e.g. charged **K** segments, with a disordered, non-ionic hydrophilic component. While there are a few candidate water soluble, disordered, non-ionic polypeptides,[25] we chose to use segments based on water soluble poly(L-methionine sulfoxide), $\mathbf{M^O}$, as this polymer is readily prepared, avoids the need to use racemic amino acid monomers, and is a naturally occurring residue that shows minimal toxicity.[26-28]

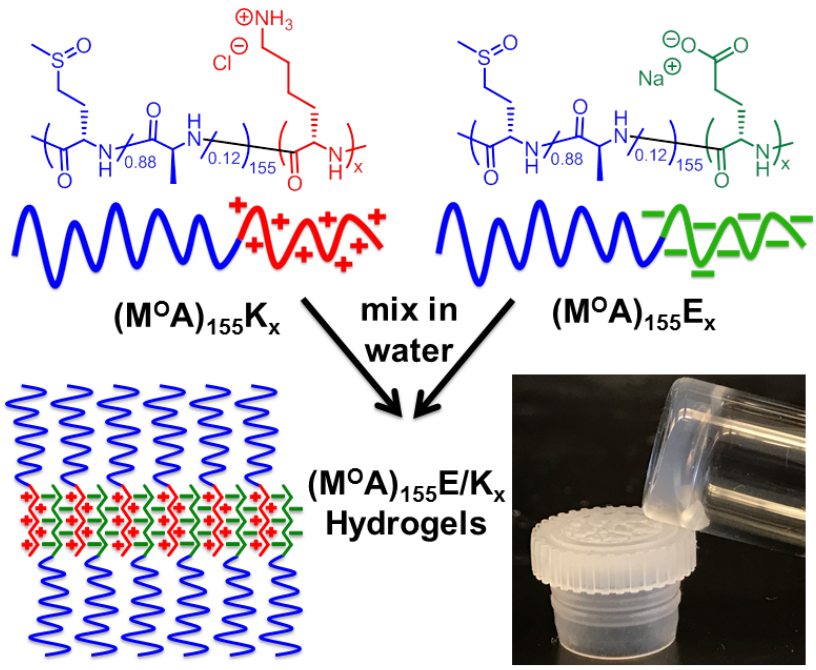

Figure 1. Schematic showing assembly process for preparation of polyion complex $\mathbf{(M^OA)_{155}E/K_x}$ diblock copolypeptide hydrogels.

Results and Discussion

Candidate DCH_{PIC} compositions were designed to include long, disordered hydrophilic segments as well as oppositely charged ionic segments able to form β-sheet complexes upon mixing (Figure 1). For shorter chain lengths (*ca*. 60 residues), non-ionic, hydrophilic $\mathbf{M^O}$ segments have been conveniently prepared from poly(L-methionine), **M**, precursors by post-polymerization oxidation.[28] However, at longer chain lengths, i.e. >100 residues, **M** polymers aggregate during polymerization, which limits the ability to control chain length and prepare well-defined block copolymers.[29] This issue was circumvented by mixing a small amount of L-alanine N-carboxyanhydride (NCA) monomer (*ca*. 12 mol %) with L-methionine NCA to prepare statistical copolymer segments that did not aggregate during polymerization due to disrupted side-chain packing.[29] The incorporation of a small amount of minimally hydrophobic alanine was found to allow efficient copolypeptide synthesis without adversely affecting

the water solubility or disordered conformation of the resulting poly(L-methionine sulfoxide-*stat*-L-alanine), $\mathbf{M^{O}A}$, segments compared to $\mathbf{M^{O}}$ homopolymer (see SI Figure S13).[26,28]

Using this strategy, we prepared diblock copolypeptides containing poly(L-methionine-*stat*-L-alanine), **MA**, segments *ca*. 155 residues long, followed by side-chain protected **K** or **E** segments of different length (Scheme 1).[16,28] Subsequent oxidation of **M** residues, followed by side-chain deprotection of **K** and **E** residues and purification gave the target copolypeptides poly(L-methionine sulfoxide-*stat*-L-alanine)$_{155}$-*block*-poly(L-lysine-HCl)$_x$, $\mathbf{(M^{O}A)_{155}K_x}$; and poly(L-methionine sulfoxide-*stat*-L-alanine)$_{155}$-*block*-poly(L-glutamate-Na)$_x$, $\mathbf{(M^{O}A)_{155}E_x}$, where x = 30, 60, 90, and 120 (Scheme 1). All copolymers were isolated in high yield with compositions that closely matched expected values (see SI Table S1). The $\mathbf{M^{O}A}$ segment length was chosen based on values known, from previous studies on amphiphilic DCH,[16] to be sufficiently long to promote hydrogel formation. The **K** and **E** lengths were varied in order to study the role of structured PIC domain size on hydrogel formation and properties.

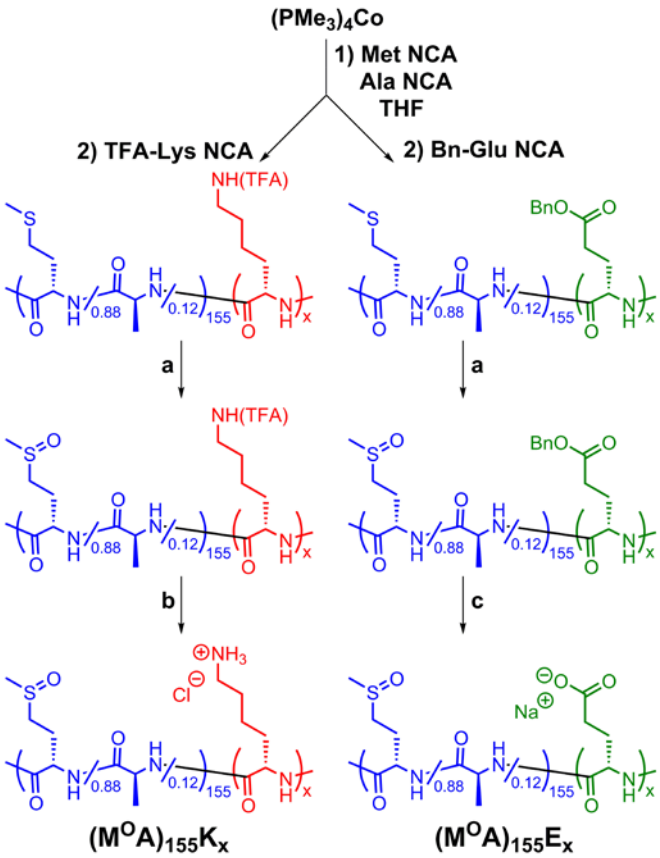

Scheme 1. Synthesis of oppositely charged, dual hydrophilic diblock copolypeptides $\mathbf{(M^{O}A)_{155}K_x}$ and $\mathbf{(M^{O}A)_{155}E_x}$. a) TBHP, CSA, H_2O, 20 °C, 1 d. b) K_2CO_3, MeOH/H_2O, 50 °C, 8 h. c) MSA, TFA, anisole, 20 °C, 1.5 h.

For initial evaluation, matching length $\mathbf{(M^{O}A)_{155}K_x}$ and $\mathbf{(M^{O}A)_{155}E_x}$ samples were separately dissolved in aqueous 1x PBS buffer (5.0 wt% of each copolypeptide) to give clear solutions. These solutions were then combined in equal volumes at essentially stoichiometric **E** to **K** ratios (*ca*. 1.02-1.04 to 1) and agitated briefly in a vortex mixer, whereupon all samples ($\mathbf{(M^{O}A)_{155}E/K_x}$, x = 30, 60, 90, and 120; 5.0 wt% total copolypeptide after mixing) were observed to form hydrogels within 15 seconds to 1 minute. These observations were confirmed by oscillatory rheology measurements where storage moduli (G') were found to dominate over loss moduli (G"), indicating elastic behavior for all samples (Figure 2A, see SI Table S2).[16] Mismatched mixtures, prepared either using non-stoichiometric **E** to **K** ratios, or by maintaining **E** to **K** stoichiometry but combining samples of different length (e.g. three $\mathbf{(M^{O}A)_{155}K_{30}}$ to one $\mathbf{(M^{O}A)_{155}E_{90}}$), were found to give substantially weaker hydrogels compared to corresponding stoichiometric and length-matched samples. Stoichiometric hydrogels prepared using longer $\mathbf{E/K_x}$ segments (90 and 120) were opaque, likely due to microscopic aggregate precipitation. Hydrogels prepared using shorter $\mathbf{E/K_x}$ segments (30 and 60) were translucent, with only slight turbidity. In general, hydrogel stiffness (G') was found to increase with $\mathbf{E/K_x}$ segment length, yet aggregate precipitation with longer segments diminished this trend, as can be seen in G' for the $\mathbf{E/K_{90}}$ sample (Figure 2A). The minimum total copolypeptide concentration required for hydrogel formation was found to be *ca*. 4.0 wt% for the $\mathbf{(M^{O}A)_{155}E/K_{30}}$ sample, and decreased with increasing $\mathbf{E/K_x}$ segment length.

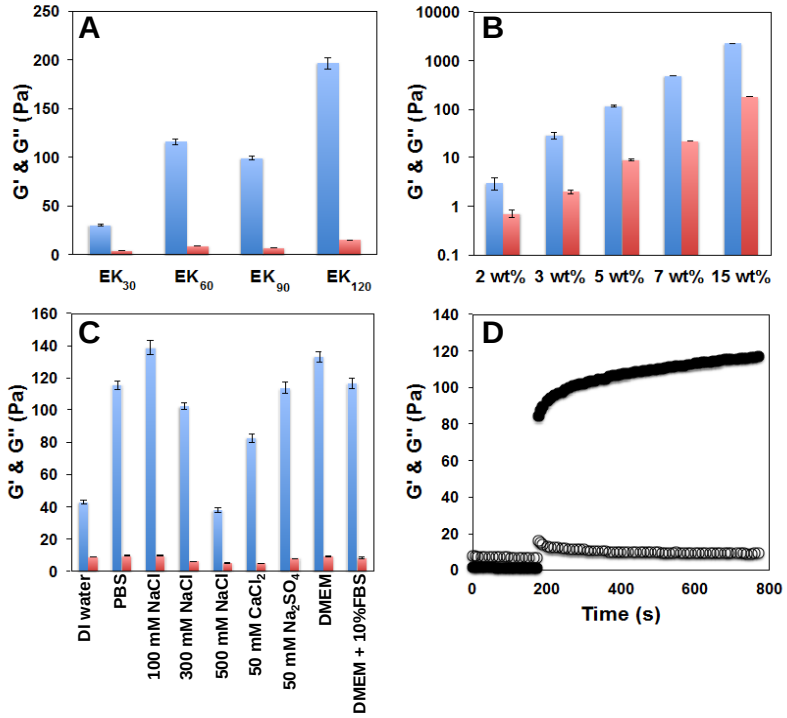

Figure 2. PIC diblock copolypeptide hydrogel properties. (A) Storage modulus, G' (Pa, blue), and loss modulus, G" (Pa, red), of hydrogels formed from stoichiometric $\mathbf{(M^OA)_{155}E/K_x}$ with different ionic segment lengths (x = 30, 60, 90, and 120). Samples (5.0 wt % total combined cationic and anionic copolypeptide) were prepared in 1x PBS buffer at 20 °C. (B) G' (Pa, blue) and G" (Pa, red), of $\mathbf{(M^OA)_{155}E/K_{60}}$ hydrogels at different concentrations in PBS buffer at 20 °C. (C) G' (Pa, blue) and G" (Pa, red), of 5.0 wt % $\mathbf{(M^OA)_{155}E/K_{60}}$ hydrogels prepared in different buffers at 20 °C. DMEM = Dulbecco's Modified Eagle Medium; FBS = fetal bovine serum. For (A, B, D), all G' and G" values were measured at an angular frequency of 5 rad/s and strain amplitude of 0.05. (D) Recovery of 5.0 wt % in PBS $\mathbf{(M^OA)_{155}E/K_{60}}$ hydrogel properties (G', filled circles; G", open circles) over time after large amplitude oscillatory breakdown (strain amplitude of 10 at 5 rad/s for 200 s), followed by linear recovery measurement (strain amplitude of 0.05 at 5 rad/s).

Due to its desirable combination of hydrogel stiffness and minimal turbidity, $\mathbf{(M^OA)_{155}E/K_{60}}$ was chosen as an optimized DCH_{PIC} composition for further study. Preparation of hydrogels using

different concentrations of **$(M^OA)_{155}E/K_{60}$** in 1x PBS was found to be a convenient means to adjust hydrogel stiffness (Figure 2B). All samples formed elastic hydrogels of similar clarity (G' » G" over a range of frequency, See SI Figure S14), and their stiffness was found to increase with higher copolypeptide concentrations. The lack of visible aggregates in these samples suggests that polymer chains were able to assemble into the desired structures even with fast mixing at high concentrations. Since the precursor solutions of two-component DCH_{PIC} are low viscosity liquids, it is noteworthy that these hydrogels can be readily prepared at significantly higher concentrations relative to one-component, amphiphilic DCH, where dissolution of copolypeptide at higher concentration (i.e. > 5.0 wt%) is hindered by spontaneous gel formation.[16] **$(M^OA)_{155}E/K_{60}$** hydrogels could also be prepared in a variety of aqueous media (Figure 2C). Solution ionic strengths in the range of *ca*. 100 to 300 mM were found to be superior for PIC hydrogel formation, while deionized water and higher salt concentrations (e.g. 500 mM NaCl) resulted in weaker hydrogels. For 5.0 wt % **$(M^OA)_{155}E/K_{30}$** in 500 mM NaCl, a hydrogel did not form, and for 5.0 wt % **$(M^OA)_{155}E/K_{90}$**, hydrogels were able to form up to 1 M NaCl, but did not form in 2 M NaCl. These results suggest that lack of charge screening in pure water prevents annealing of PIC chains into ordered complexes (*vide infra*), while conversely excess charge screening in higher salt concentrations leads to weakened complexation, and is PIC length dependent.[5,6] Finally, elevated temperature (80 °C for 1.5 h) was found to have no visible effect on a 5.0 wt% **$(M^OA)_{155}E/K_{60}$** hydrogel in 1x PBS, showing that DCH_{PIC} possess good thermal stability.

The self-healing properties of DCH_{PIC} after mechanical breakdown were studied by subjecting a 5.0 wt% **$(M^OA)_{155}E/K_{60}$** sample in 1x PBS to high amplitude oscillatory strain, and then monitoring the recovery of elasticity over time by measuring G' at a much smaller strain amplitude (Figure 2D). During the initial 200 s of high strain amplitude, G' dropped by two orders of magnitude to below the level of G", indicating the sample had become a viscous liquid. Upon switching to low strain amplitude, the sample began recovering its elastic properties, with most of the original gel stiffness regained within the

brief period (*ca*. 10 s) needed to switch between strain amplitudes. Full recovery of DCH_{PIC} elasticity continued to occur over a time scale of minutes. The rapid self-healing ability of DCH_{PIC}, which allows delivery of DCH_{PIC} via injection through small bore needles, is remarkably similar to that observed in amphiphilic DCH, such as $\mathbf{K_{180}L_{20}}$ or $\mathbf{K_{160}V_{40}}$, despite their substantial differences in chemical composition and mode of assembly.[16] The observed similarity in physical properties may arise from the modular design of these block copolymers that likely leads to formation of similar supramolecular assembled structures.

To better understand the assembly of DCH_{PIC}, the influence of polyelectrolyte chirality on hydrogel formation was studied. We designed DCH_{PIC} such that the **K** and **E** segments were envisioned to form structured PICs, rich in β-sheet content, upon complexation.[7,9,10] To test this hypothesis, a new copolypeptide component, $\mathbf{(M^OA)_{155}(}\boldsymbol{rac}\mathbf{\text{-}E)_{60}}$, was prepared, where the ***rac*-E** segment was composed of racemic residues that should inhibit β-sheet formation in PICs.[5-7,22] When equivalent amounts of $\mathbf{(M^OA)_{155}(}\boldsymbol{rac}\mathbf{\text{-}E)_{60}}$ and $\mathbf{(M^OA)_{155}K_{60}}$ were mixed (total 5.0 wt% in 1x PBS), the resulting sample did not form a hydrogel and gave only a low viscosity liquid (see SI Figure S15). This result confirmed the importance of chirality in formation of $\mathbf{(M^OA)_{155}E/K_{60}}$ hydrogel structure. To directly verify the formation of β-sheet assembly in $\mathbf{(M^OA)_{155}E/K_x}$ DCH_{PIC}, the hydrogels were also analyzed using FTIR, since different polypeptide conformations possess characteristic stretching frequencies for their Amide I and Amide II bands.[30] In FTIR analysis of lyophilized $\mathbf{(M^OA)_{155}E/K_x}$ hydrogels (x = 30, 60, 90, and 120), all samples possessed strong 1653 cm^{-1} Amide I bands due to the disordered chain conformations of the $\mathbf{(M^OA)_{155}}$ segments (see SI Figures S13,S16). The samples also possessed 1630 cm^{-1} Amide I bands, characteristic of β-sheet chain conformations, which increased in intensity as $\mathbf{E/K_x}$ segment length increased suggesting that this band resulted from PIC formation (see SI Figure S16). The β-sheet Amide I band at 1630 cm^{-1} was only present in the homochiral $\mathbf{(M^OA)_{155}E/K_x}$ PICs, and was absent in the individual components as well as the $\mathbf{(M^OA)_{155}(}\boldsymbol{rac}\mathbf{\text{-}E)/K_{60}}$ PIC formed with a racemic component

(see SI Figure S17). Together, these data confirmed that the **K** and **E** segments in $\mathbf{(M^{O}A)_{155}E/K_x}$ PIC are assembling as β-sheets, and that this organized assembly is required for hydrogel formation.

The supramolecular structure of $\mathbf{(M^{O}A)_{155}E/K_{60}}$ hydrogels was analyzed at both microscale and nanoscale resolution. To visualize microscopic structure, chains of $\mathbf{(M^{O}A)_{155}E_{60}}$ and $\mathbf{(M^{O}A)_{155}K_{60}}$ were separately conjugated with different fluorescent probes (tetramethylrhodamine and fluorescein, respectively) and then mixed to form DCH_{PIC}. Laser scanning confocal microscopy (LSCM) was then used to visualize the labeled chains and the hydrogel network (Figure 3A,B). Both **K** labeled (TRITC, red) and **E** labeled (FITC, green) channels showed DCH_{PIC} are composed of microporous networks containing interconnected polypeptide rich domains that coexist with domains primarily composed of water, seen as dark regions in the images.[31] An overlay of red and green channels revealed that **K** and **E** segments are co-localized, indicating good mixing of the components within the DCH_{PIC} domains (Figure 3C). Cryo electron microscopy (cryoEM) imaging of a thin layer of vitrified $\mathbf{(M^{O}A)_{155}E/K_{60}}$ hydrogel showed structures resembling "plumber's nightmare" morphologies, which consist of membrane like regions interconnected with tape-like struts, and contain many defects that form a nanoporous network (Figure 3D). The combination of microscale and nanoscale structure in DCH_{PIC} is reminiscent of structure observed in amphiphilic DCH. [16] The design of DCH_{PIC} appears to have been successful in mimicking amphiphilic DCH by replicating many of their structural features and properties even though DCH_{PIC} utilize PICs instead of hydrophobic segments for self-assembly.

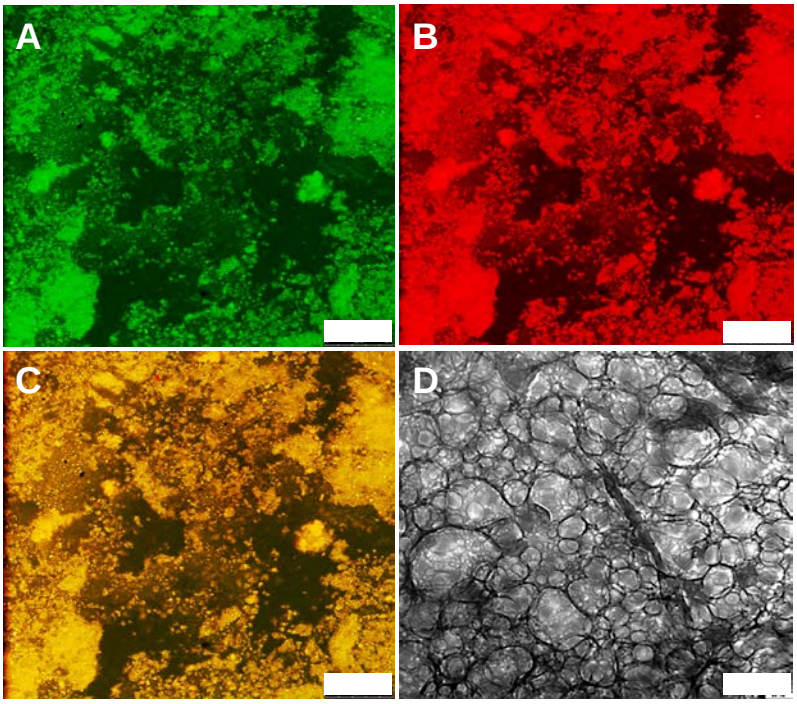

Figure 3. Laser scanning confocal and cryoelectron microscopy (cryoEM) images of $\mathbf{(M^{O}A)_{155}E/K_{60}}$ hydrogels. (A,B,C) LSCM images (z-thickness = 0.78 μm) of TRITC labeled $\mathbf{(M^{O}A)_{155}K_{60}}$ (red) and FITC labeled $\mathbf{(M^{O}A)_{155}E_{60}}$ (green) hydrogel mixtures showing microporous structure (3.0 wt% in PBS). (A) FITC channel; (B) TRITC channel; (C) Merge of A and B. (D) CryoEM image of $\mathbf{(M^{O}A)_{155}E/K_{60}}$ hydrogel showing nanoporous structure (2.0 wt% in PBS). Scale bars: A,B,C = 25 μm; D = 200 nm.

Compared to amphiphilic DCH, DCH_{PIC} were found to possess a significant difference in hydrogel stability against dilution in aqueous media. Amphiphilic DCH are formed by direct dissolution of solid copolypeptide in aqueous media, where samples, e.g. $\mathbf{K_{180}L_{20}}$, swell to fill the volume and spontaneously form hydrogels. If additional media is then added, the copolypeptides will continue to disperse to give diluted samples that fill the larger volume.[16] While this property allows facile preparation of DCH formulations for a number of applications, [32] it does limit the ability to suspend hydrogels in excess media, as could be desired for *in vitro* cell culture.[33] To study the stability of DCH_{PIC} against dilution in aqueous media, a 5.0 wt% $\mathbf{(M^{O}A)_{155}E/K_{60}}$ hydrogel in PBS was prepared, and then an equal volume of DMEM cell culture media was added on top of the hydrogel (Figure 4A).

For comparison, a similar experiment was performed using a 2.0 wt% $\mathbf{K_{180}L_{20}}$ hydrogel in PBS (Figure 4B), where its concentration was chosen to match the stiffness of the $\mathbf{(M^OA)_{155}E/K_{60}}$ hydrogel. Initially, the DMEM solutions formed clear layers above both hydrogels. After 3 days, the $\mathbf{K_{180}L_{20}}$ sample had fully mixed with the DMEM layer and the diluted sample was a viscous liquid. With $\mathbf{(M^OA)_{155}E/K_{60}}$, although the DMEM solutes were able to diffuse into the sample over 3 days, the hydrogel was able to retain its shape and stiffness (Figure 4C,D). Compared to the hydrophobic interactions of amphiphilic DCH, the combination of H-bonding and electrostatic interactions present in the assemblies of DCH_{PIC} was found to impart superior resistance against dissolution in aqueous media.

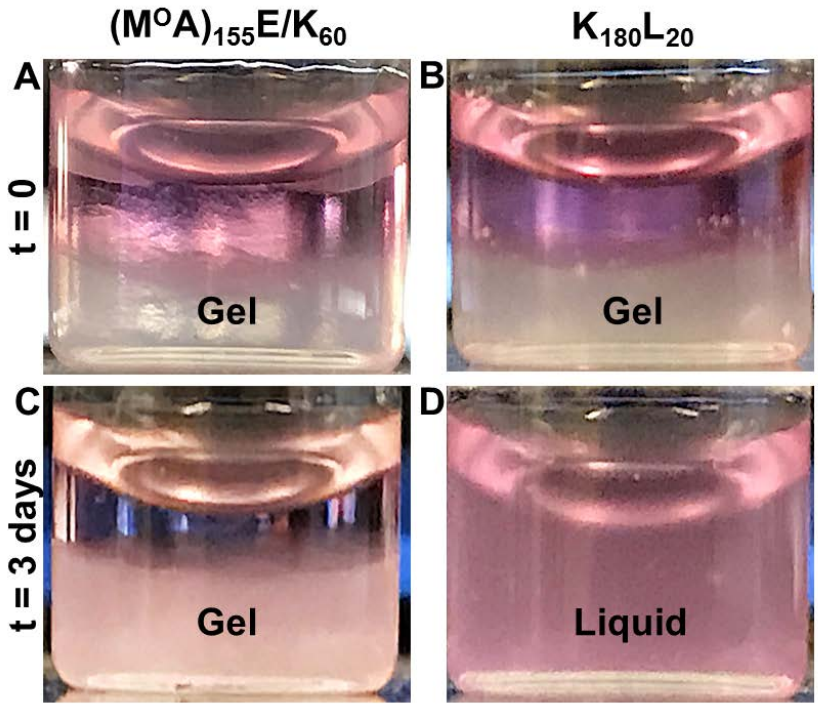

Figure 4. Stability of diblock copolypeptide hydrogels against dilution. Polyion complex $\mathbf{(M^OA)_{155}E/K_{55}}$ (A and C, 5.0 wt%) and hydrophobic assembled $\mathbf{K_{180}L_{20}}$ (B and D, 2.0 wt%) hydrogels of equivalent stiffness (G' ≈ 120 Pa) in 1x PBS were each diluted with an equal volume of DMEM cell culture media. (A,B) A layer of cell media formed over both gels at the beginning of the experiment

(time = 0). (C,D) After 3 days, the **$(M^{O}A)_{155}E/K_{60}$** hydrogel remained intact, while **$K_{180}L_{20}$** had dispersed into the full volume of media and was a liquid.

The ability of DCH_{PIC} to resist dissolution or swelling once formed provides a means to cast hydrogel shapes from precursor solutions, and then use these stable hydrogels for various applications in aqueous media. To showcase their potential utility, we encapsulated primary neural stem progenitor cells (NSPCs)[33] in a **$(M^{O}A)_{155}E/K_{60}$** hydrogel (Figure 5). The NSPCs were encapsulated by mixing a suspension of cells in media with an equal volume of **$(M^{O}A)_{155}E_{60}$** solution in media, which was then combined with an equal volume of **$(M^{O}A)_{155}K_{60}$** solution in media to rapidly form the cell containing hydrogel. This sample, as well as cell only and cell in **$K_{180}L_{20}$** hydrogel controls in media, was incubated for 1 day, and then cell viability was quantified using a Live/Dead assay (Figure 5).[34] The cationic **$K_{180}L_{20}$** hydrogel was found to be highly cytotoxic, as expected from the literature,[33] and served as a good negative control. The **$(M^{O}A)_{155}E/K_{60}$** hydrogel provided good cell viability, similar to the cells in media only control, which suggests that DCH_{PIC} may be promising for use a cell carrier. Although DCH_{PIC} contain long, charged polypeptide segments, these are effectively sequestered by PIC formation and steric shielding from the uncharged **$M^{O}A$** hydrophilic segments, resulting in hydrogels that are effectively non-ionic.[35] Although cells were exposed to the non-complexed, charged components of DCH_{PIC} during the mixing process, this brief exposure, regardless of mixing order, was found to have minimal adverse effects on cell viability. More detailed studies on cell suspension in DCH_{PIC} will be the subject of future investigations.

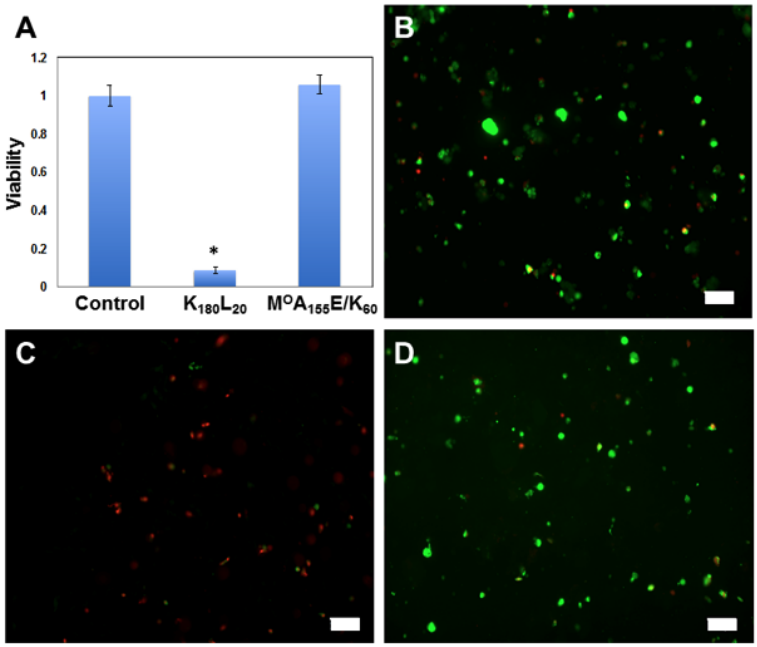

Figure 5. Viability of neural stem progenitor cells (NSPCs) encapsulated in hydrogels. (A) Plot of NSPC viability after 1 day incubation in different conditions: cells in media only control, in media plus 2.0 wt% $\mathbf{K_{180}L_{20}}$ hydrogel, or in media plus 5.0 wt% $\mathbf{(M^OA)_{155}E/K_{60}}$ hydrogel. (B-D) Fluorescence microscopy images of NSPC cells after 1 day incubation under different conditions and then stained using the Live/Dead® viability/cytotoxicity assay where green is due to calcein (live cells) and red is due to EthD-1 (dead cells). (B) cells in media only control. (C) cells in media plus 2.0 wt% $\mathbf{K_{180}L_{20}}$ hydrogel. (D) cells in media plus 5.0 wt% $\mathbf{(M^OA)_{155}E/K_{60}}$ hydrogel. Scale bars = 100 μm. * $p<0.0001$ (Unpaired student's t-test for $\mathbf{K_{180}L_{20}}$ with either cell control or $\mathbf{(M^OA)_{155}E/K_{60}}$).

Conclusions

A new class of cell-compatible copolypeptide hydrogels, DCH_{PIC}, that possess chain conformation directed PIC supramolecular architectures was reported. The use of polypeptide components that form β-sheets upon polyion complexation, in combination with non-ionic disordered segments, led to anisotropic supramolecular assembly into anisotropic structures that form extended

hydrogel networks capable of rapid self-healing after deformation. Unlike amphiphilic DCH, the use of PIC assembly in DCH_{PIC} was found to impart these materials with stability against dilution in aqueous media, a valuable feature for downstream applications. While there are many examples of useful materials based on liquid coacervate or disordered PIC assemblies, the promising attributes and unique features of DCH_{PIC} highlight the potential for use of conformational order in PIC assembly to create new supramolecular materials.

Associated Content

Supporting Information

The Supporting Information is available free of charge on the ACS Publications website at DOI: 10.1021/jacs.#######.

Experimental procedures, spectral data, rheology data, circular dichroism spectra, and methods for all hydrogel characterization and cell culture (PDF).

Author Information

Corresponding Author

* demingt@seas.ucla.edu

ORCID

Timothy J. Deming: 0000-0002-0594-5025

Notes

The authors declare no competing financial interest.

Acknowledgments.

The authors thank Eric Raftery for assistance with ATR-IR measurements, and Professor Pirouz Kavehpour and Kelly Connelly for access to equipment and assistance with rheology measurements. This work was supported by the Dr. Miriam and Sheldon G. Adelson Medical Research Foundation and NSF (DMR-1548924 to ZHZ). The authors acknowledge the use of instruments at the Electron Imaging Center for NanoMachines supported by NIH (1S10RR23057) and CNSI at UCLA.

References.

1) Boekhoven, J.; Stupp, S. I. *Adv. Mater.* **2014**, *26*, 1642–1659.

2) Webber, M. J.; Appel, E. J.; Meijer, E. W.; Langer, R. *Nat. Mater.* **2016**, *15*, 13-26.

3) Woolfson, D. N. in *Fibrous Proteins: Structures and Mechanisms*, *Subcellular Biochemistry 82*, Parry, D. A. D.; Squire, J. M. (eds.), Springer: Cham, Switzerland, **2017**, 35-61.

4) Deming, T. J., Ed. *Top. Curr. Chem.* **2012**, *310*, 1 – 171.

5) Blocher, W. C.; Perry, S. L. *WIREs Nanomed. Nanobiotechnol.* **2017**, *9*, e1442.

6) Marciel, A. B.; Chung, E. J.; Brettmann, B. K.; Leon, L. *Adv. Coll. Interface Sci.* **2017**, *239*, 187–198.

7) Perry, S. L.; Leon, L.; Hoffmann, K. Q.; Kade, M. L.; Priftis, D.; Black, K. A.; Wong, D.; Klein, R. A.; Piercel II, C. F.; Margossian, K. O.; Whitmer, J. K.; Qin, J.; de Pablo, J. J.; Tirrell, M. *Nat. Commun.* **2015**, *6*, 6052, DOI: 10.1038/ncomms7052.

8) Priftis, D.; Leon, L.; Song, Z.; Perry S. L.; Margossian, K. O.; Tropnikova, A.; Cheng, J.; Tirrell, M. *Angew. Chem. Int. Ed.* **2015**, *54*, 11128 –11132.

9) Blout, E. R.; Idelson, M. *J. Amer. Chem. Soc.* **1958,** *80*, 4909-4913.

10) Hammes, G. G.; Schullery, S. E. *Biochemistry* **1968,** *7*, 3882-2887.

11) Pacalin, N. M.; Leon, L.; Tirrell, M. *Eur. Phys. J. Special Topics* **2016**, *225*, 1805–1815.

12) Lemmers, M.; Sprakel, J.; Voets, I. J.; van der Gucht, J.; Cohen Stuart, M. A. *Angew. Chem. Int. Ed.* **2010**, *49*, 708 –711.

13) Hunt, J. N.; Feldman, K. E.; Lynd, N. A.; Deek, J.; Campos, L. M.; Spruell, J. M.; Hernandez, B. M.; Kramer, E. J.; Hawker, C. J. *Adv. Mater.* **2011**, *23*, 2327–2331.

14) Cui, H.; Zhuang, X.; He, C.; Wei, Y.; Chen, X. *Acta Biomater.* **2015**, *11*, 183–190.

15) Chassenieux, C.; Tsitsilianis, C. *Soft Matter*, **2016**, *12*, 1344-1359.

16) Nowak, A. P.; Breedveld, V.; Pakstis, L.; Ozbas, B.; Pine, D. J.; Pochan, D.; Deming, T. J. *Nature* **2002,** *417*, 424-428.

17) Yoon, H.; Dell, E. J.; Freyer, J. L.; Campos, L. M.; Jang, W-D. *Polymer* **2014**, *55*, 453-464.

18) Harada, A.; Kataoka, K. *Macromolecules* **1996**, *28*, 5294-5299.

19) Harada, A.; Kataoka, K. *Science* **1999**, *283*, 65-67.

20) Koide, A.; Kishimura, A.; Osada, K.; Jang, W-D.; Yamasaki, Y.; Kataoka, K. *J. Amer. Chem. Soc.* **2006**, *128*, 5988-5989.

21) Anraku, Y.; Kishimura, A.; Oba, M.; Yamasaki, Y.; Kataoka, K. *J. Amer. Chem. Soc.* **2010**, *132*, 1631-1636.

22) Mutaf, O. F.; Kishimura, A.; Mochida, Y.; Kim, A.; Kataoka, K. *Macromol. Rapid Commun.* **2015**, *36*, 1958−1964.

23) Wu, L. C.; Yang, J.; Kopeček, J. *Biomaterials* **2011**, *32*, 5341-5353.

24) Rombouts, W. H.; de Kort, D. W.; Pham, T. T .H.; van Mierlo, C. P. M.; Werten, M. W. T.; de Wolf, F. A.; van der Gucht, J. *Biomacromolecules* **2015**, *16*, 2506−2513.

25) Deming, T. J. *Chem. Rev.* **2016**, *116*, 786–808.

26) Aiba, S-I.; Minoura, M.; Fujiwara, Y. *Makromol. Chem.* **1982**, *183*, 1333-1342.

27) Pitha, J.; Szente, L.; Greenberg, J. *J. Pharmaceutical Sci.* **1983**, *72*, 665-668.

28) Rodriguez, A. R.; Kramer, J. R.; Deming, T. J. *Biomacromolecules* **2013**, *14*, 3610-3614.

29) Kramer, J. R.; Deming, T. J. *Biomacromolecules* **2010**, *11*, 3668-3672.

30) Miyazawa, T. in *Poly-α-amino acids Protein models for conformational studies*, Fasman, G. D. (ed.), Dekker: New York, New York, **1967**, 69-104.

31) Srivastava, S.; Andreev, M.; Levi, A. E.; Goldfeld, D. J.; Mao, J.; Heller, W. T.; Prabhu, V. M.; de Pablo, J. J.; Tirrell, M. *Nat. Commun.* **2017**, *8*, 14131, DOI: 10.1038/ncomms14131.

32) Anderson, M. A.; Burda, J. E.; Ren, Y.; Ao, Y.; O'Shea, T. M.; Kawaguchi, R.; Coppola, G.; Khakh, B. S.; Deming, T. J.; Sofroniew, M. V. *Nature* **2016**, *532*, 195-200.

33) Zhang, S.; Burda, J. E.; Anderson, M. A.; Zhao, Z.; Ao, Y.; Cheng, Y.; Sun, Y.; Deming, T. J.; Sofroniew, M. V. *ACS Biomater. Sci. Eng.* **2015**, *1*, 705-717.

34) Cheng, T.; Chen, M.; Chang, W.; Huang, M.; Wang, T. *Biomaterials*, **2013**, *34*, 2005-2016.

35) Black, K. A.; Priftis, D.; Perry, S. L.; Yip, J.; Byun, W. Y.; Tirrell. M. *ACS Macro Lett.* **2014**, *3*, 1088−1091.

TOC graphic

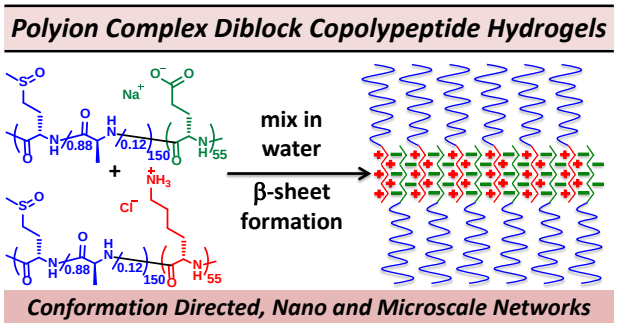
Polyion Complex Diblock Copolypeptide Hydrogels
mix in water
β-sheet formation
Conformation Directed, Nano and Microscale Networks